

Potassium Phthalocyanine, KPC: One-Dimensional Molecular Stacks Bridged by K⁺ Ions

Serena Margadonna,^{*,†} Kosmas Prassides,^{*,‡} Yoshihiro Iwasa,^{*,§} Yasujiro Taguchi,[§] Monica F. Craciun,^{||} Sven Rogge,^{||} and Alberto F. Morpurgo^{||}

School of Chemistry, University of Edinburgh, Edinburgh EH9 3JJ, U.K., Department of Chemistry, University of Durham, Durham DH1 3LE, U.K., Institute for Materials Research, Tohoku University, Sendai 980-8577, Japan, CREST—Japan Science and Technology Agency, Kawaguchi 332-0012, Japan, and Kavli Institute of Nanoscience, Delft University of Technology, NL-2628CJ Delft, The Netherlands

Received April 28, 2006

We report the synthesis of potassium phthalocyanine (KPC) and its structural characterization by synchrotron X-ray powder diffraction. We find that while KPC adopts the β -polymorphic structural type (monoclinic space group $P2_1/a$) common for many MPC solids, its structure is characterized by unique features. The K⁺ ions, which are statistically disordered over two symmetry-equivalent positions, reside in the intrastack spacing of the rodlike molecular assemblies and strongly bond equidistantly to selected N atoms of the two neighboring Pc rings along the chain direction with an unusual 5-fold coordination. The K⁺-stuffed slipped stacks of Pc units display much greater intrastack and slippage distances than those of other β -MPC polymorphs. They may be thought as comprising disordered dimeric (Pc)₂²⁻ units; this leads to electron pairing and is consistent with the observed nonmagnetic response of the system.

Introduction

Metallophthalocyanines, MPC's, form a rich family of multifunctional materials that display diverse catalytic, optical, electronic, and magnetic properties, studied widely over many years.¹ These materials are invariably built up in the solid state by quasi-one-dimensional slipped stacks of planar Pc macrocycles. Adjacent stacks interact weakly and are typically inclined with respect to each other at an angle of 90°. In divalent transition-metal Pc's, MPC (M = Mn–Zn), the metal ions reside at the center of the macrocycle, coordinating to four N atoms and retaining D_{4h} molecular point group symmetry. A number of polymorphic forms of MPC are encountered in the solid state, differing by the mode of intrastack packing as well as the relative interchain

orientations. The most stable crystalline form is usually that of the β -polymorph,² in which the tilting angle, defined as the angle between the stacking direction and the normal to the plane of each molecule, is about 45°. For divalent metal ions like Mg²⁺, the metal cation is somewhat shifted off the center of the macrocycle, resulting in nonplanar MgPc molecules with C_{4v} point group symmetry.³

Because of the good electron-donating ability of the MPC molecules, hole-doped MPC solids have long been known to form an archetypal family of molecular metals.⁴ In these systems, controlled oxidation of the MPC units is achieved, for example, by iodination to afford highly conducting molecular materials, characterized by a face-to-face stacking architecture of the metal macrocycles, which ensures strong uniaxial π – π orbital overlap.^{4,5} Very recently, we have embarked on a research program of exploring the chemistry

* To whom correspondence should be addressed. E-mail: serena.margadonna@ed.ac.uk (S.M.), K.Prassides@durham.ac.uk (K.P.), iwasa@imr.tohoku.ac.jp (Y.I.).

[†] University of Edinburgh.

[‡] University of Durham.

[§] Tohoku University and CREST—Japan Science and Technology Agency.

^{||} Delft University of Technology.

(1) (a) Leznoff, C. C.; Lever, A. B. P. *Phthalocyanines: Properties and Applications*; VCH: New York, 1997; Vols. 1–4. (b) McKeon, N. B. *Phthalocyanine Materials*; Cambridge University Press: Cambridge, U.K., 1998.

(2) (a) Mason, R.; Williams, G. A.; Fielding, P. E. *J. Chem. Soc., Dalton Trans.* **1979**, 676. (b) Figgis, B. N.; Kucharski, E. S.; Williams, G. A. *J. Chem. Soc., Dalton Trans.* **1980**, 1515. (c) Figgis, B. N.; Mason, R.; Williams, G. A. *Acta Crystallogr., Sect. B* **1980**, *36*, 2963.

(3) (a) Janczak, J.; Kubiak, R. *Polyhedron* **2001**, *20*, 2901. (b) Mizuguchi, J. *J. Phys. Chem. A* **2001**, *105*, 1121. (c) Mizuguchi, J. *J. Phys. Chem. A* **2001**, *105*, 10719.

(4) (a) Marks, T. J. *Angew. Chem.* **1990**, *29*, 857. (b) Inabe, T.; Tajima, H. *Chem. Rev.* **2004**, *104*, 5503.

and characterizing the physical properties of hitherto unknown electron-doped MPC assemblies.⁶ Electron doping into MPC to afford phases with stoichiometry $A_x[\text{MPC}]$ (A = alkali metal) has been achieved by means of reactions with alkali metals using a variety of synthetic protocols. In the course of such exploratory chemical procedures, we were also able to isolate the alkali-metal Pc phase, KPc, whose structural and physical characterizations are reported in this paper.

LiPc is the only alkali-metal Pc phase known at present.⁷ It has attracted very wide interest because it represents an example of a neutral radical crystal with intrinsic semiconducting properties, composed of a monovalent metal and a monoanionic Pc radical ligand.^{4b} LiPc is a planar molecular system, with Li^+ residing strictly in the center of the Pc ring cavity. Three polymorphic (α , β , and x) LiPc forms have been structurally characterized in the solid state,⁸ and their magnetic and electrical properties⁹ have been studied extensively. Here we report that the structural and electronic properties of the KPc analogue are drastically different. KPc crystallizes with the β -polymorphic structure but shows no evidence for paramagnetic behavior expected for a neutral radical solid.¹⁰ Although it is formally isostructural with β -LiPc, replacement of Li^+ by K^+ leads to marked changes in the intrastack packing motif because the Pc units slip relative to each other along the stacking direction and the K^+ ions move significantly away from the plane of the Pc rings inside the intrastack spacing.

Experimental Details

The KPc samples used in the present work were synthesized by reacting a CuPc powder with an excess amount (4:1) of K in a sealed glass tube under vacuum (5×10^{-6} Torr) for 48 h. Prior to the reaction, as-purchased CuPc powder was purified in a thermal gradient by vacuum sublimation. All sample manipulations were undertaken in an Ar-atmosphere glovebox (oxygen concentration ≈ 1 ppm). The CuPc powder was loaded into one end of the

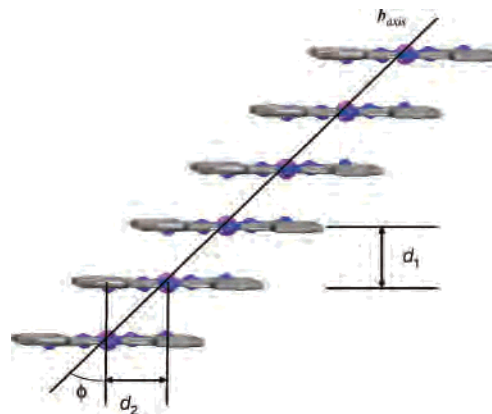


Figure 1. Slip-stacked MPC assemblies along the crystallographic b axis that make up the monoclinic (space group $P2_1/a$) crystal structure of the β -polymorphs of MPC solids ($M = \text{Li}$, divalent transition metal).

reaction tube, which was kept at 450 °C, while the K metal was introduced at the other end of the tube, which was heated to 200 °C. Products with different compositions were condensed at different positions of the walls of the reaction tube (Supporting Information, Figure 1S). Material collected from the bottom of the tube near the CuPc end was found to be phase pure, as confirmed by X-ray powder diffraction, which also revealed the presence of elemental Cu metal. High-resolution synchrotron X-ray diffraction measurements were performed on powdered samples sealed in 0.5-mm-diameter glass capillaries. Data were collected at ambient temperature with an image-plate detector on the BL02B2 beamline ($\lambda = 1.0008$ Å; $2\theta = 3$ – 50°) at SPring-8, Hyogo, Japan. One-dimensional diffraction patterns were obtained by integrating around the rings using local software. Analysis of the diffraction data was performed with the GSAS suite of Rietveld analysis programs.

Raman spectra of powdered samples sealed in capillaries were measured at ambient temperature using a micro-Raman spectrometer with an excitation wavelength of 633 nm. For IR absorption measurements of the sample, we prepared a KPc-dispersed KBr pellet and introduced it in a sealed cell equipped with ZnSe windows for IR light in an Ar-filled glovebox to avoid any degradation due to air exposure. The IR absorption spectra of the sample were then measured using a Fourier transform (FT)-IR spectrometer (Jasco FT-IR/4200). Following these measurements, we removed the sample from the sealed cell and recorded its IR spectra as a function of time following exposure to air. Magnetization curves were recorded at 2 K on samples (~ 4.2 mg) sealed in quartz tubes with a Quantum Design SQUID magnetometer. The background contributions from the quartz tubes were subtracted. X-band electron paramagnetic resonance (EPR) experiments were performed on samples sealed in quartz capillaries in the temperature range from 4 to 300 K. The magnetic susceptibility was determined by double integration of the EPR signal followed by calibration with the response measured for 1,1-diphenyl-2-picrylhydrazyl radicals diluted in a Y_2O_3 powder. The g value of the EPR signal was determined by comparison with a standard Mn^{2+} sample.

Results

Structural Analysis. The β -polymorphs of MPC's typically adopt monoclinic structures (space group $P2_1/a$: $a = 19.49$ Å, $b = 4.81$ Å, $c = 14.64$ Å, and $\beta = 121.1^\circ$ for CuPc) in which the planar metallomacrocycles form stacks along the short b axis of the unit cell (Figure 1).² The synchrotron X-ray powder diffraction profile of the present

- (5) (a) Schramm, C. J.; Scaringe, R. P.; Stojakovic, D. R.; Hoffman, B. M.; Ibers, J. A.; Marks, T. J. *J. Am. Chem. Soc.* **1980**, *102*, 6702. (b) Yakushi, K.; Yamakado, H.; Yoshitake, M.; Kosugi, N.; Kuroda, H.; Sugano, T.; Kinoshita, M.; Kawamoto, A.; Tanaka, J. *Bull. Chem. Soc. Jpn.* **1989**, *62*, 687. (c) Ogawa, M. Y.; Hoffman, B. M.; Lee, S.; Yudkowsky, M.; Halperin, W. P. *Phys. Rev. Lett.* **1986**, *57*, 1177. (d) Thompson, J. A.; Murata, K.; Durcharne, R.; Poirier, M.; Hoffman, B. M. *Phys. Rev. B* **1999**, *60*, 523. (e) Martin, I.; Phillips, P. *Phys. Rev. B* **1999**, *60*, 530.
- (6) (a) Craciun, M. F.; Rogge, S.; den Boer, M. J. L.; Margadonna, S.; Prassides, K.; Iwasa, Y.; Morpurgo, A. F. *Adv. Mater.* **2006**, *18*, 320. (b) Craciun, M. F.; Rogge, S.; Morpurgo, A. F. *J. Am. Chem. Soc.* **2005**, *127*, 12210. (c) Taguchi, Y.; Miyake, T.; Margadonna, S.; Kato, K.; Prassides, K.; Iwasa, Y. *J. Am. Chem. Soc.* **2006**, *128*, 3313.
- (7) (a) Homborg, H.; Kalz, W. *Z. Naturforsch. B: Anorg. Chem. Org. Chem.* **1978**, *33*, 1067. (b) Sugimoto, H.; Higashi, T.; Mori, M. *J. Chem. Soc., Chem. Commun.* **1983**, 622.
- (8) (a) Sugimoto, H.; Mori, M.; Masuda, H.; Taga, T. *J. Chem. Soc., Chem. Commun.* **1986**, 962. (b) Wachtel, H.; Wittmann, J.-C.; Lotz, B.; Petit, M. A.; André, J.-J. *Thin Solid Films* **1994**, *250*, 219. (c) Homborg, H.; Teske, C. L. *Z. Anorg. Allg. Chem.* **1985**, *527*, 45.
- (9) (a) Turek, P.; André, J.-J.; Simon, J. *Solid State Commun.* **1987**, *63*, 741. (b) Dumm, M.; Lunkenheimer, P.; Loidl, A.; Assmann, B.; Homborg, H.; Fulde, P. *J. Chem. Phys.* **1996**, *104*, 5048. (c) Brinkmann, M.; Turek, P.; André, J.-J. *J. Mater. Chem.* **1998**, *8*, 675.
- (10) Solvated K_2Pc derivatives have been reported: $\text{K}_2\text{Pc}(18\text{-crown-6})_2$ and $\text{K}_2\text{Pc}(\text{diglyme})_2$ (Ziolo, R. F.; Guenther, W. H. H.; Troup, J. M. *J. Am. Chem. Soc.* **1981**, *103*, 4629) and $\text{K}_2\text{Pc}(\text{DMF})_4$ (Ziolo, R. F.; Extine, M. *Inorg. Chem.* **1981**, *20*, 2709).

reaction product obtained at ambient temperature revealed that there were no Bragg reflections corresponding to the starting CuPc material, which was therefore consumed in the course of the reaction. However, at diffraction angles higher than 27° , sharp intense reflections were evident, indexing on the face-centered-cubic unit cell of elemental Cu and therefore providing the signature of its formation as a product of the reaction between CuPc and K. All other reflections present obeyed the extinction rules of the primitive monoclinic $P2_1/a$ space group, but their angular positions were significantly shifted from those of the CuPc starting material, thereby implying a strong renormalization of the unit cell dimensions in the KPc product while the same monoclinic structure is retained. Analysis of the diffraction data with the LeBail pattern decomposition technique then proceeded smoothly, resulting in lattice parameters of $a = 16.933 \text{ \AA}$, $b = 5.929 \text{ \AA}$, $c = 13.482 \text{ \AA}$, and $\beta = 113.46^\circ$ (agreement factors: $R_{\text{wp}} = 1.83\%$, $R_{\text{exp}} = 0.74\%$). These results are consistent with K^+ intercalation into empty spaces of the generic structure of the β -polymorphs of Pc's without significantly perturbing the basic stacking architecture of the macrocycles. However, a notable feature is that the individual monoclinic lattice constants, a , b , and c , do not respond in the same way upon replacement of the transition-metal cation by K^+ : while the short axis b , which defines the stacking direction of the Pc columns, sharply increases by $\sim 23\%$, the lattice constants a and c , which reflect the magnitude of the interstack separations, sharply decrease by 13% and 8% , respectively, also accompanied by a considerable decrease in the monoclinic angle, β . The severe shortening of the separation of adjacent chains from $\sim 10 \text{ \AA}$ in CuPc to $\sim 9 \text{ \AA}$ provides the signature that K^+ is not accommodated at interstitial holes between the stacks. On the other hand, the drastic increase in the intrastack separation and the accompanying overall inflation of the unit cell volume by $\sim 5.7\%$ imply that the intercalated K^+ resides in interstitial sites within the stacks.

Rietveld refinements of the synchrotron X-ray diffraction data were then initiated using the monoclinic structural model of the β -polymorphs of transition-metal Pc's or LiPc, placing the K^+ ion at the central hole of the macrocycle and retaining the slip-stacked one-dimensional molecular columns along the short b axis, with adjacent stacks inclined by symmetry at an angle of 90° . However, the agreement between the calculated and observed diffraction profiles within this model was not satisfactory throughout the entire 2θ range ($R_{\text{wp}} = 5.84\%$). At this stage, we note that this structural model has some intrinsic unsatisfactory characteristics because it necessitates square-planar coordination of the large alkali-metal ion ($r_{\text{K}^+} = 1.33 \text{ \AA}$) and very short $\text{K}^+ - \text{N}$ ($\sim 2.0 \text{ \AA}$) contacts. Thus, starting from the previous model, we performed a search of possible alternative positions of the K^+ ion by allowing it to move off the center of the Pc ring [$2a$ ($1/2, 1/2, 0$) site of the unit cell] along a direction perpendicular to the molecular plane and monitoring the resulting quality-of-fit factors (R_{wp}) of the Rietveld refinements. The new K^+ sites [$4e$ ($1/2 + x, 1/2 + y, z$)] necessitate the splitting of each alkali ion into two symmetry-

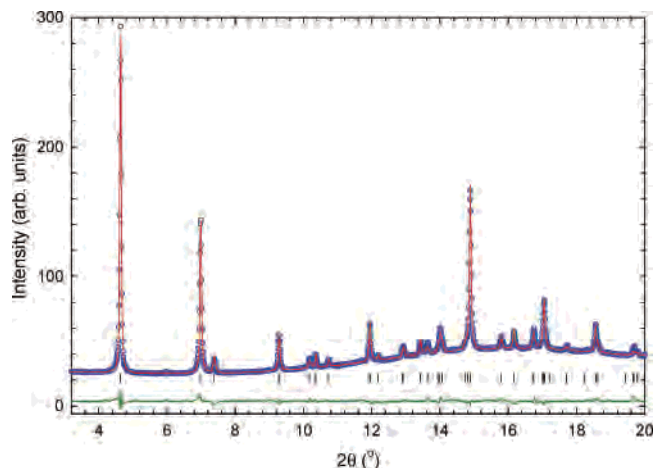


Figure 2. Final observed (○) and calculated (red solid line) powder synchrotron X-ray ($\lambda = 1.0008 \text{ \AA}$) diffraction profiles for KPc at ambient temperature. The lower green solid line shows the difference profile, and the tick marks show the reflection positions.

Table 1. Refined Position and Fractional Occupancy, n , of the K^+ Ion in KPc and Selected K–N Interatomic Distances (\AA), As Obtained by Rietveld Refinement of the Synchrotron X-ray Powder Diffraction Data at 295 K^a

atom	x/a	y/b	z/c	n
K	0.554(1)	0.647(2)	0.962(1)	0.540(5)
bond	distance	bond	distance	
K–N(1)	2.44(1)	K–N(4) $\times 2$	2.45(1)	
K–N(2) $\times 2$	2.44(1)			

^a Estimated errors in the last digits are given in parentheses.

equivalent positions, equidistantly displaced above and below the Pc ring with a fractional occupancy of $1/2$. The refinements were stable, with R_{wp} sharply decreasing as the K^+ ion was progressively displaced until its position approached a single deep minimum (at 2.82%) for $x \approx 0.05$, $y \approx 0.15$, and $z \approx -0.04$. The results of the final Rietveld refinements [lattice constants: $a = 16.9349(6) \text{ \AA}$, $b = 5.9299(2) \text{ \AA}$, $c = 13.4800(5) \text{ \AA}$, $\beta = 113.438(4)^\circ$, $V = 1242.03(3) \text{ \AA}^3$; agreement factors: $R_{\text{wp}} = 1.93\%$, $R_{\text{exp}} = 0.74\%$] after allowing the positional parameters and occupation number of the K^+ ion to vary are shown in Figure 2, with the fitted parameters and selected distances summarized in Tables 1S (Supporting Information) and 1, respectively. Refinement of the fractional occupancy of the K^+ ion resulted in a nominal stoichiometry of $\text{K}_{1.08(1)}\text{Pc}$.¹¹ The obtained crystal structure of the KPc material is shown in Figure 3.¹²

Raman and FT-IR Spectroscopic Measurements. The Raman spectra of the β -CuPc starting material and the KPc reaction product at ambient temperature in the frequency region $200\text{--}1600 \text{ cm}^{-1}$ are displayed in Figure 4. They are comparable to those reported before for β -CuPc and other

- (11) At first glance, it may appear counterintuitive that a KPc phase forms upon exposing CuPc to an excess of K vapor. We note, however, that the reaction occurs in the gas phase and condensation of KPc is accompanied by the formation of additional products with stoichiometry $\text{K}_x[\text{CuPc}]$.
- (12) In the course of the refinements, we unambiguously established that structural models comprising ordered arrangements of the K^+ ions, which would reduce the space group symmetry from $P2_1/a$ to Pa or $P2_1$, led to inferior quality of fit to the experimental data.

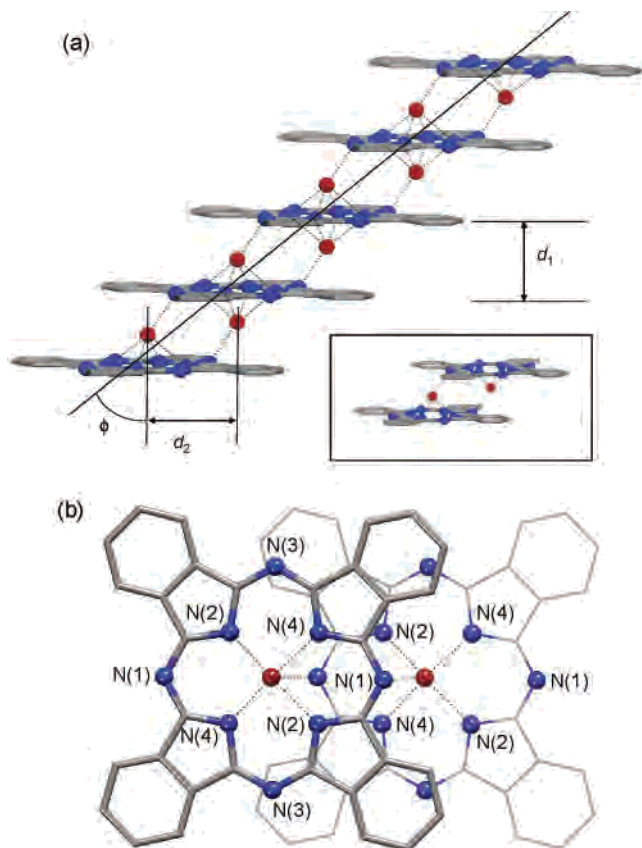


Figure 3. (a) Slip-stacked Pc assembly along the b axis in KPc ($d_1 = 3.41$ Å; $d_2 = 4.85$ Å; $\phi = 54.9^\circ$). K^+ ions (depicted in red) are disordered and reside exclusively in the intrastack spacing, bonding strongly to N atoms of two neighboring Pc units (dotted lines). The inset shows the $[K_2Pc_2]$ building block of the one-dimensional assemblies. (b) Projection of two neighboring Pc molecules within the same stack along the direction normal to their planar rings in KPc, emphasizing their increased relative slippage when compared to the usual β -polymorphic MPc structures.

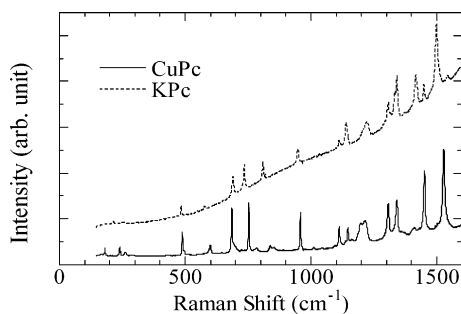


Figure 4. Raman spectra of powder samples of β -CuPc (solid line) and KPc (dotted line).

transition-metal phthalocyanines $M^{\text{II}}Pc$.^{13,14} Although both the β -CuPc and KPc spectra are very similar to each other, implying that the Pc ring is not greatly modified following the replacement of Cu^{2+} by the K^+ ion, a systematic shift in the positions of most of the observed vibrational modes is evident. Expanded regions of the Raman spectra in the frequency range of the most intense vibrational modes are shown in Figure 5, where the detailed changes are more

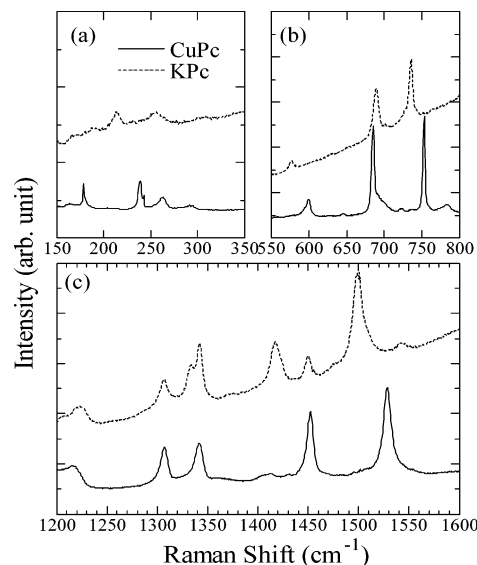


Figure 5. Expanded regions of the Raman spectra of β -CuPc (solid line) and KPc (dotted line): (a) 150–350 cm^{-1} ; (b) 550–800 cm^{-1} ; (c) 1200–1600 cm^{-1} .

clearly visible. For instance, Figure 5c reveals a softening of the $B_{1g}(D_{4h})/B_1(C_{4v})$ vibrational frequency from 1529 cm^{-1} in CuPc to 1499 cm^{-1} in KPc, consistent with the change in the charge state of the Pc ring upon substitution of Cu^{2+} by K^+ . Other notable peaks are those observed at 239 and 263 cm^{-1} in CuPc, which also show downshifts to 214 and 255 cm^{-1} , respectively, upon substitution. These bands have been assigned before¹³ to vibrational modes involving displacements of the central metal ion, and thus they should be particularly sensitive to its identity. The observed frequency downshifts may be understood in terms of the reduction in force constants that accompanies the change in the charge state of the central metal ion from divalent to monovalent, despite the reduction in atomic mass. Frequency shifts of varying magnitude are also present in other energy regions of the spectra (Figure 5 and Table 2S in the Supporting Information) and should be presumably related to both the shift in position of the central metal atom with respect to the Pc ring and the change in the charge state of the Pc ring upon substitution of Cu^{2+} by K^+ .

The IR spectrum of a KPc sample in a sealed cell is shown in Figure 6 together with that of β -CuPc. They are comparable to those reported for transition-metal phthalocyanines $M^{\text{II}}Pc$.¹⁵ A comparison between the β -CuPc and KPc spectra provides a picture similar to that described above for the Raman spectra; namely, while they are very similar to each other, there are systematic shifts in the positions of most of the observed vibrational modes (Figure 6, inset). We also followed the evolution of the IR spectrum of the KPc sample with exposure time to the atmosphere (Figure 2S in the Supporting Information). Well-defined changes that saturate after ~ 1 h are evident, implying sensitivity of the as-synthesized KPc material to air exposure. The most notable changes include a frequency shift of the modes around

(13) (a) Tackley, D. R.; Dent, G.; Smith, W. E. *Phys. Chem. Chem. Phys.* **2000**, *2*, 3949. (b) Tackley, D. R.; Dent, G.; Smith, W. E. *Phys. Chem. Chem. Phys.* **2001**, *3*, 1419.

(14) Basova, T. V.; Kolesov, B. A. *J. Struct. Chem.* **2000**, *41*, 770.

(15) (a) Yakushi, K.; Yamakado, H.; Ida, T.; Ugawa, A. *Solid State Commun.* **1991**, *78*, 919. (b) Hiejima, T.; Yakushi, K. *J. Chem. Phys.* **1995**, *103*, 3950.

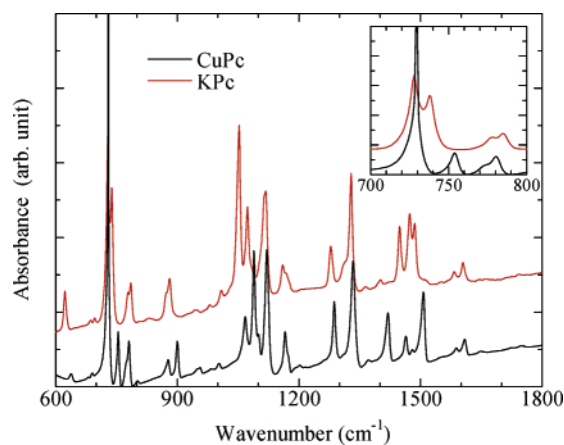


Figure 6. IR spectra of β -CuPc (black line) and KPc unexposed to air (red line). Inset: Expanded region of the spectra in the range 700–800 cm^{-1} .

1000–1100 cm^{-1} immediately after the sample was exposed to air, the gradual growth of a broad peak around 1400 cm^{-1} , and the emergence of a new vibrational mode at 1640 cm^{-1} .

Magnetization and EPR Measurements. Figure 7 shows the field-dependent magnetization curves recorded at 2 K for β -CuPc and KPc. The CuPc data are well described by a Brillouin function with a saturation magnetization corresponding to a $S = 1/2$ system. In contrast, the magnetization of KPc is drastically reduced at 2 K, consistent with the loss of paramagnetic spins at 2 K. It is 1 order of magnitude smaller than that of CuPc, corresponding to an apparent concentration of only 0.07 spin $1/2$ centers per molecule at 2 K.

The X-band EPR spectra of CuPc and KPc at room temperature are displayed in Figure 8. The g value is 2.052(2) for CuPc, consistent with the observed spins being attributed to d spins of the Cu^{2+} ion at the center of the Pc macrocycle. On the other hand, the g value extracted from the KPc EPR spectrum is 2.003(1) and can be attributed to π spins, possibly associated with the Pc ring. More importantly, the integrated intensity of the ESR signal of KPc, which is a measure of the spin susceptibility, is drastically smaller than that of β -CuPc. Figure 9 summarizes the temperature dependence of the spin susceptibility, χ , and of the full width at half-maximum (fwhm) of the EPR resonance curve. The middle panel of Figure 9 shows a plot of the inverse spin susceptibility, χ^{-1} , vs temperature. The observed almost linear T dependence indicates that the unpaired spins follow a standard Curie law behavior with a negligibly small Weiss constant. From the value of the Curie constant, the spin density can be calculated as $5 \times 10^{-4} \text{ mol}^{-1}$. This extremely small value of the spin density indicates that the observed π -electron spins correspond to paramagnetic impurities or defects. Such an interpretation is also supported by the almost temperature-independent fwhm of the EPR signal. Therefore, the EPR data show unambiguously that, unlike LiPc, which is a paramagnetic π -radical crystal, KPc is nonmagnetic.

Discussion

All monoclinic β -polymorphic forms of transition-metal phthalocyanines, MPc ($M = \text{Mn}–\text{Zn}$), adopt essentially

identical crystalline structures in which the planar metallo-macrocycles form slip-stacked one-dimensional columns along the short b axis with an interplanar separation, d_1 , on the order of 3.2 Å (Figure 1).² The slipped packing motif of the MPc molecules is such that two pyrrole-bridging N(1) atoms of each Pc unit lie at ~ 3.2 Å almost directly above or below the M^{II} ions of its two nearest neighbors [$M–N(1)\cdots M \approx 90^\circ$]. As a result, each M^{2+} ion coordinates strongly to four equatorial N atoms of the same molecule at ~ 2 Å and weakly to two apical N(1) atoms from adjacent molecules along the stack at a longer distance, thereby leading to an overall pseudo-octahedral bonding environment. These weak intermolecular interactions are crucial in stabilizing the β -polymorphic structures, while their importance is also manifested in peculiarities of the MPc electronic structure; for instance, the origin of the intrachain ferromagnetic interactions in β -MnPc can be traced to the ferromagnetic exchange interactions between the Mn d orbitals on one MnPc unit and those in neighboring units via a 90° superexchange pathway mediated by the p orbitals of the nearest-neighbor N(1) atoms.^{6c,16} In addition, the same intermolecular $M\cdots N(1)$ interactions have been invoked as the driving force for the rationalization of the stability of the nonplanar structure of the MgPc molecules in solid MgPc;³ namely, as the Mg^{2+} ion shifts out of the Pc ring by ~ 0.4 Å toward the neighboring N(1) atoms, it adopts a [4 + 1] coordination with four short intramolecular $M–N$ bonds of length ~ 2.0 Å and one longer intermolecular $M\cdots N(1)$ bond of ~ 2.7 Å.

The structural results for the KPc system have proven sufficiently accurate to provide a detailed comparison of its structure with those of M^{II} Pc and LiPc solids. First, while KPc remains formally isostructural with an identical quasi-one-dimensional slip-stacked packing architecture of the Pc units, the short chain axis b increases markedly from ~ 4.8 to ~ 5.9 Å (Figure 3). This difference in structural chemistry is associated with the fact that the large K^+ ion has moved away from the center of the Pc ring and is exclusively accommodated within the intrastack spacing. Each K^+ ion is disordered with a 50% occupancy factor over the two interstitial sites shown in Figure 3 and is displaced from the Pc plane by 1.48 Å. It is remarkable that this interstitial equilibrium position (Table 1), as determined by the Rietveld refinements, is such that the bonding distances of every K^+ ion to the four isoindole N atoms of the Pc molecule and to the pyrrole-bridging N(1) atom of the neighboring Pc ring are the same within experimental error at ~ 2.45 Å (Figure 3). These $\text{K}^+–\text{N}$ distances are comparable to those encountered in coordination complexes of K^+ with NH_3 in ammoniated alkali-metal fullerene¹⁷ and graphite¹⁸ intercalates and imply strong bonding interactions of K^+ with all five of its

- (16) (a) Barraclough, C. G.; Martin, R. L.; Mitra, S.; Mitra, S. *J. Chem. Phys.* **1970**, *53*, 1638. (b) Miyoshi, H.; Ohya-Nishiguchi, H.; Deguchi, Y. *Bull. Chem. Soc. Jpn.* **1973**, *46*, 2724. (c) Mitra, S.; Gregson, A. K.; Hatfield, W. E.; Weller, R. R. *Inorg. Chem.* **1983**, *22*, 1729. (d) Awaga, K.; Maruyama, Y. *Phys. Rev. B* **1991**, *44*, 2589.
- (17) (a) Rosseinsky, M. J.; Murphy, D. W.; Fleming, R. M.; Zhou, O. *Nature* **1993**, *364*, 425. (b) Margadonna, S.; Prassides, K.; Shimoda, H.; Takenobu, T.; Iwasa, Y. *Phys. Rev. B* **2001**, *64*, 132414.
- (18) Solin, S. A. *J. Phys., Paris IV* **1991**, *C5*, 311.

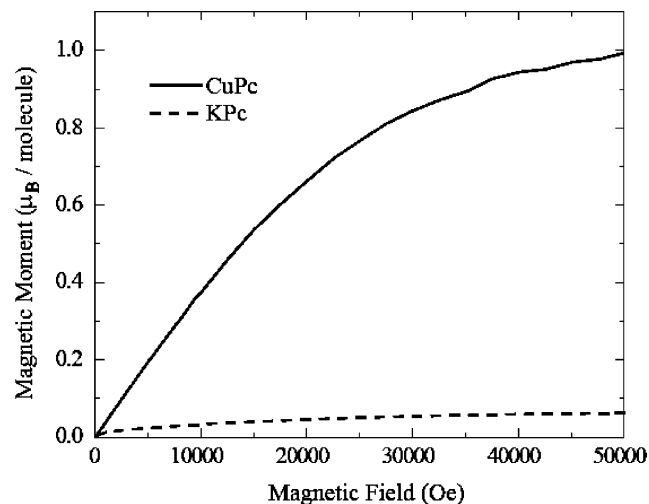


Figure 7. Magnetic field dependence of the magnetization of β -CuPc and KPc crystalline powders recorded at 2 K.

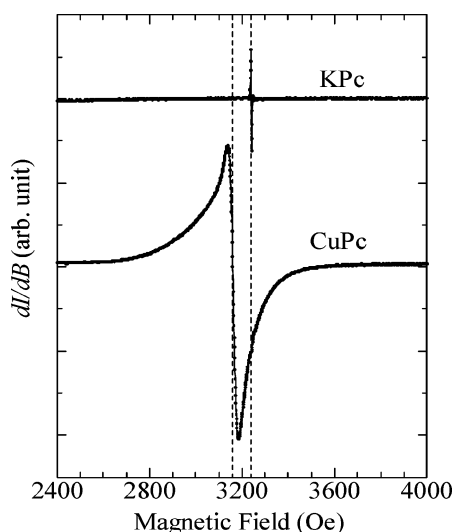


Figure 8. X-band EPR spectra of β -CuPc and KPc crystalline powders at room temperature.

neighboring N atoms in an unusual 5-fold coordination. This is distinctly different from the Mg–N coordination in MgPc, where there is a clear differentiation between intramolecular and intermolecular contacts.

Finally, it is noticeable in the KPc solid that, although the intrastack separation changes drastically by $\sim 23\%$, the separation between neighboring planar Pc molecules, d_1 , increases much less (only by $\sim 6\%$ from ~ 3.2 to ~ 3.41 Å). Instead, the Pc units allow for accommodation of the K^+ ions in the intrastack spacing by increasing their slipping distance relative to each other along the stacking direction (Figure 10). This results in an increased slipping distance, d_2 , of the stacks to ~ 4.85 Å and an opening up of their slipping angle, ϕ , to $\sim 55^\circ$. The increased slippage of the stacks is crucial in removing steric hindrance between the K^+ ions and near-neighboring Pc units along the stacking direction, while at the same time the lack of off-axis ions leads to a contraction (to ~ 9 Å) of the separation of adjacent KPc chains.

We now turn our attention to the discussion of the magnetic properties of KPc, drawing from the detailed

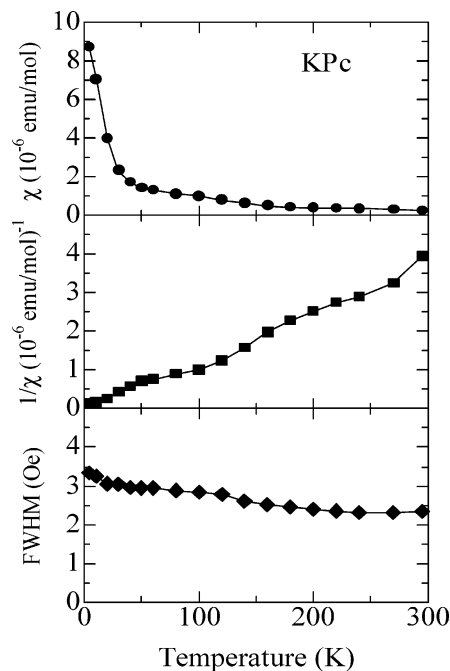


Figure 9. Temperature dependence of (top) the spin susceptibility, χ , determined from the integrated intensity of the X-band EPR spectra of KPc, (middle) the inverse susceptibility, χ^{-1} , and (bottom) the fwhm of the EPR signal.

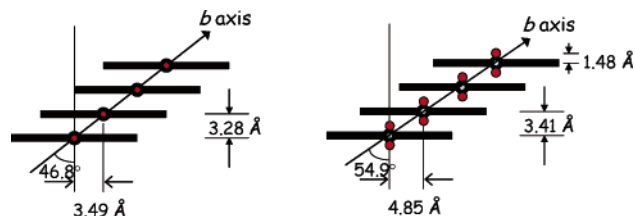


Figure 10. Schematic representation of the molecular packing arrangement along the one-dimensional stacks in β -MPc (left panel) and KPc (right panel).

structural results. Formally KPc can be formulated as a neutral radical salt in analogy with LiPc. The β -polymorph of LiPc, in which the Li^+ ion resides strictly at the center of the macrocycle, shows paramagnetic behavior characteristic of a spin $1/2$ system with strong antiferromagnetic coupling (Weiss temperature = -60 K).⁹ Its magnetic behavior is complex, differing between powders and needle crystals, and is influenced by the presence of defects and adsorbed O_2 . On the other hand, as evidenced by both the magnetization and the EPR data, the KPc solid is nonmagnetic and the observed narrow EPR line arises from a very low concentration of residual paramagnetic defects (~ 1 spin per 2000 Pc units). It thus appears that the unpaired spins of the $Pc^{\cdot -}$ radicals do not contribute to the magnetic response.

Several features of the peculiarities of the KPc structure may be responsible for the suppression of magnetism in this system. First, we note that the isostructural MgPc solid in which the Mg^{2+} ion is also located outside the Pc plane (0.4 Å) has been described as being comprised of $(MgPc)_2$ dimers that are statistically disordered along the stack axis.³ A similar description is also very appealing in the present case, especially because the off-plane displacement of the K^+ ions is significantly more pronounced (1.48 Å), leading

to an equidistant 5-fold coordination with four equatorial N atoms of every Pc molecule and an apical N_a atom of its neighbor. The presence of such statistically disordered (Pc)₂²⁻ dimers (Figure 3a, inset) running along the chains and bonded strongly together by the K⁺ ions could naturally account for the electron pairing and the absence of a paramagnetic response. In addition, given that each K⁺ ion is strongly bound to the two Pc rings, the electronic structure of the molecular Pc units is strongly perturbed. Because of the formation of strong K⁺–N(1) bonding, the charge density distribution of the donated electrons by the K atoms is not fully delocalized over each macrocyclic skeleton as in LiPc and MPc (M = transition metal) but also is strongly localized in the vicinity of the N(1) atoms of its neighbors. These combined effects seem to lead to Pc^{•-} radical units binding to each other in pairs, thereby resulting in the disappearance of paramagnetism in the present system.

Conclusions

In conclusion, we have isolated and structurally characterized the β -polymorph of KPc. The large K⁺ ion is disordered over two symmetry-equivalent positions and moves substantially off the center of the Pc ring along the direction perpendicular to the molecular plane. This is accompanied by a significant renormalization of the molecular stacking

architecture along the slipped-stacking direction of the Pc columns, which accommodate the alkali-metal ion guests by a combination of expanded intrastack distances and increased molecular slippage. Remarkably, in the resulting equilibrium structure, the K⁺ ions are equidistantly sandwiched between two Pc molecules and are found to bond strongly with four isoindole N atoms of one Pc ring and a pyrrole-bridging N(1) atom of the other. These structural and bonding motifs give rise to disordered dimeric (Pc)₂²⁻ units along the chain direction bridged by the K⁺ ions and should be responsible for the observation that KPc is nonmagnetic and therefore not a neutral π -radical system.

Acknowledgment. We thank SPring-8 for synchrotron X-ray beamtime. This work was supported by the Daiwa Foundation (to K.P. and Y.I.) and the Royal Society (Dorothy Hodgkin Research Fellowship to S.M.).

Supporting Information Available: Figures of the reaction tube setup in the course of the synthetic procedure and of the time dependence of the IR spectrum of KPc following exposure to air and tables of the Rietveld refinement parameters and the observed Raman frequencies. This material is available free of charge via the Internet at <http://pubs.acs.org>.

IC060727+